# Influence of the composition and preparation of the rotating disk electrode on the performance of mesoporous electrocatalysts in the alkaline oxygen reduction reaction

# Influence of the composition and preparation of the rotating disk electrode on the performance of mesoporous electrocatalysts in the alkaline oxygen reduction reaction

Nick Daems,[a,b] Tom Breugelmans,[b] Ivo F.J. Vankelecom,[a] and Paolo P. Pescarmona*[a,c]

**Abstract:** We report a systematic study of the influence of the composition and preparation method of the electrocatalyst layer deposited on the rotating (ring-)disk electrodes (RDE/RRDE) employed in the alkaline oxygen reduction reaction (ORR). In order to investigate and rationalise the generally underestimated role of these factors on the ORR performance of mesoporous electrocatalyts, we studied the activity and selectivity of a nitrogen-doped ordered mesoporous carbon (NOMC) as a function of the loading of electrocatalyst and of binder, of the type of binder and of the addition order of the components onto the electrode. The use of an anion-exchange polymer (Fumion FAA-3®) as binder instead of the commonly employed Nafion® increased the selectivity towards $H_2O_2$ while leading to lower kinetic current density. On the other hand, higher selectivity towards $H_2O$ was observed upon increase in the loading of the catalyst and of the binder, although the latter resulted in decreased kinetic current density. These results prove the crucial effect of the composition and preparation method of the layer deposited on the electrode on the ORR performance of the mesoporous electrocatalyst and can provide useful guidelines in view of the translation of the results of RDE-studies to an alkaline fuel cell set-up.

[a] Dr. N. Daems, Prof. Dr. I.F.J. Vankelecom, Prof. Dr. P.P. Pescarmona
Centre for Surface Chemistry and Catalysis
KU Leuven
Celestijnenlaan 200F, 3001 Heverlee, Belgium
[b] Dr. N. Daems, Prof. Dr. T. Breugelmans
Advanced Reactor Technology
U Antwerpen
Campus Drie Eiken, Universiteitsplein 1, 2610 Wilrijk, Belgium
[c] Prof. Dr. P.P. Pescarmona
Chemical Engineering Group
Engineering and Technology Institute Groningen (ENTEG)
Universtity of Groningen
Nijenborgh 4, 9747 AG Groningen, The Netherlands
E-mail: p.p.pescarmona@rug.nl

Supporting information for this article is given via a link at the end of the document.

## Introduction

In recent years, research about renewable energy sources has experienced a considerable boost, mainly due to the rising societal awareness concerning greenhouse gas emissions and their environmental impact. Another important factor driving this research is the fossil fuel depletion.[1] In this context, increasing research endeavours focuses on proton exchange membrane fuel cells (PEMFCs) that generate electricity by exploiting the energy liberated by the electrochemical reduction of oxygen coupled to the oxidation of hydrogen. However, the commercialisation of these fuel cells is still hampered by the high cost and the poor stability of the Pt-based oxygen reduction reaction (ORR) electrocatalysts. These limitations stimulated the search for alternative electrocatalysts for the ORR with lower Pt loadings or, preferably, devoid of noble metals.[2–8]

Initially, the attempts mainly focused on pyrolysed carbon-supported transition metal complexes, but neither the stability nor the activity of these electrocatalysts reached the desired levels. Eventually this research further shifted to metal-free doped carbon materials, which reached similar ORR performance to the Pt-based electrodes in alkaline environments, while displaying much higher long-term stability. In acidic environment, they are not yet competitive enough with Pt-based electrodes.[9–12] Both in acidic and in alkaline environment, the reduction of $O_2$ to $H_2O$ can occur either through a direct mechanism involving the transfer of four electrons (1) or via a sequential mechanism with hydrogen peroxide as an intermediate (2).

$$O_2 + 4H^+ + 4e^- \longrightarrow 2H_2O \quad (pH< 7) \quad E^\circ = 1.23\ V$$
$$O_2 + 2H_2O + 4e^- \longrightarrow 4OH^- \quad (pH> 7) \quad E^\circ = 0.40\ V \qquad (1)$$

$$O_2 + 2H^+ + 2e^- \longrightarrow H_2O_2 \quad (pH< 7) \quad E^\circ = 0.70\ V$$
$$O_2 + H_2O + 2e^- \longrightarrow HO_2^- + OH^- \quad (pH> 7) \quad E^\circ = -0.08\ V \qquad (2.A)$$

$$H_2O_2 + 2H^+ + 2e^- \longrightarrow 2\ H_2O \quad (pH< 7) \quad E^\circ = 1.78\ V$$
$$HO_2^- + H_2O + 2e^- \longrightarrow 3\ OH^- \quad (pH> 7) \quad E^\circ = 0.87\ V \qquad (2.B)$$

If the sole purpose of the fuel cell is to generate electricity, an ideal electrocatalyst should promote the complete reduction with formation of water as final product. In this context, the formation of $H_2O_2$ is considered a drawback as it lowers the current generated per oxygen molecule. Furthermore, the decomposition of $H_2O_2$ releases radicals, which are known to damage the Nafion® membranes commonly applied in PEMFCs.[13–18] On the other hand, hydrogen peroxide is an industrially relevant chemical product (worldwide annual production of 3.8 million tonnes[19]) that can be used as a green oxidant in a broad range of applications.[20] Therefore, the selective reduction of $O_2$ to $H_2O_2$ can also be attractive from an economic point of view since it would allow cogeneration of electricity and of an industrially important commodity product.[2]

Due to the existence of Nafion® (a sulphonated fluoropolymer based on a tetrafluoroethylene backbone) as a commercially available, high-performance proton-exchange membrane, PEMFCs are the fuel cells that have received the most attention thus far. However, since it has been discovered that alkaline fuel cells allow the use of a much broader range of electrocatalytic materials for the ORR,[13] there has been an increased interest towards alkaline ORR and anion exchange membranes.[4,21]-[24]

The expected impact of fuel cells and the challenges summarised above explain the growing research efforts dedicated to the development of enhanced electrocatalysts for the ORR.[4,11,24–27] Generally, the performance of novel electrocatalysts in the ORR is first investigated with a rotating disk electrode (RDE) or a rotating ring-disk electrode (RRDE)in a half-cell setup.[28] Both the RDE and the RRDE techniques allow determining the onset potential, the half-wave potential ($E_{1/2}$) and the kinetic current density ($J_K$), which provide an assessment of the activity of the electrocatalyst. With the RRDE technique, the selectivity can be determined directly from the experiments based on a comparison of the ring and the disk current. The RDE uses

the Koutécky-Levich equations to estimate the selectivity[28] based on the number of exchanged electrons (*n*). For both techniques, the measurement conditions are a crucial factor influencing the performance of the tested electrocatalysts. This influence can be so relevant as to lead to contradictory results (especially for the selectivity) for the same electrocatalyst.[3,29] Important factors influencing the electrocatalytic performance are the scan rate (at higher rates slower reactions might be inhibited), the electrolyte type and concentration (acidic vs. alkaline; KOH vs. NaOH)[30] and, most critically, the composition of the catalyst ink and the preparation of the electrode.[31,32] The influence of the ink composition (e.g. solvent, binder content,[33] catalyst content[17,29] and duration of sonication) and of the electrode manufacturing (e.g. amount of ink added,[17] drying temperature and atmosphere) on the ORR behaviour were investigated for different electrocatalysts consisting of metal particles supported on a porous material on a RDE. These studies demonstrated the major influence of the loading of porous electrocatalysts on their ORR performance. Several studies have shown that the selectivity towards water increases with the loading of porous electrocatalyst. This can be rationalised considering that at higher loadings the electrocatalyst layer is thicker and the produced $H_2O_2$ has to travel a larger distance through the porous structure prior to its release in the electrolyte: therefore, the probability to encounter another active site that promotes its further reduction to water increases.[16,17,29,34] However, if the ORR follows the direct four electron reduction mechanism, the amount of $H_2O_2$ that is generated should be insensitive to the catalyst loading since every $O_2$ molecule is adsorbed and reduced on the same active site without leaving it. By varying the catalyst loading, it is thus possible to discriminate between the direct four electron reduction and the sequential mechanism with $H_2O_2$ as an intermediate.[35] This effect is specific of porous electrocatalysts, in opposition to conventional electrocatalysts consisting of an ideal flat surface. Another important factor is the binder content, which is typically an ionomer (e.g. Nafion®) that acts as binder for fixing the electrocatalyst on the glassy carbon support in the RDE and RRDE. The binder loading should be sufficiently high to prevent the electrocatalyst from falling off at high rotation speeds, though very high loadings should be avoided too, since they could block all the access paths of oxygen to the active sites.[13,36] A more recent study showed that also the electrical conductivity of the electrocatalyst itself has an impact on the selectivity. By varying the conductivity of a perovskite oxide or by adding different amounts of a conductive carbon, it was shown that a more conductive environment resulted in a higher selectivity towards water ($4e^-$-pathway).[37]

Although the role of some of the parameters involved in the RDE fabrication has already been explored for Pt-based electrocatalysts,[38] for non-noble metal-containing electrocatalysts[17] and $CN_x$ materials,[29,32] a systematic study of all the relevant parameters is still lacking.

Moreover, no study so far addressed the effect of these parameters for the newer and very promising class of metal-free, porous electrocatalysts, of which N-doped ordered mesoporous carbons (NOMCs) are one of the most relevant examples. Therefore, we decided to study and rationalise the influence of the composition and fabrication method of the electrocatalyst layer on a NOMC that was previously developed by our group and that exhibited excellent activity and selectivity as electrocatalyst for the cogeneration of electricity and hydrogen peroxide in an alkaline fuel cell.[2] The choice of a NOMC as test electrocatalyst in this study is further motivated by its ordered porous structure and high specific surface area, which can grant accessibility to the active species also when a high catalyst loading is used on the RDE surface. This feature distinguishes doped ordered mesoporous carbons from other electrocatalysts that do not present a network of pores going through the material (e.g. from conventional electrodes consisting of a single metal surface but also from metal particles supported on a low surface area material as graphite). A final reason for studying NOMCs is that very similar materials from this class have been reported to display very different selectivity in the ORR, with values of *n* either very close to 2 ($H_2O_2$ as main product) or 4 ($H_2O$ as main product).[2,21] Therefore, a study of the effect of composition and preparation of the electrocatalyst layer on the ORR performance of NOMCs is particularly timely.

The impact of this work can go beyond RDE-based electrochemical studies and can prove relevant also when applying the best performing (porous) electrocatalysts identified by RDE techniques in membrane electrode assemblies (MEA), which are evaluated in complete fuel cells. Although the use of RDE (and RRDE) for the initial screening and ranking of different electrocatalysts is widely accepted, significant discrepancies have been often observed between the performance of electrocatalysts measured with RDE and that of the same materials in a MEA.[39] Differences in the composition and fabrication method of the electrocatalyst layer in the RDE and in the MEA areconsidered among the main causes of these discrepancies. Therefore, understanding the influence of the composition and preparation method of the electrocatalyst layer in the RDE on its performance can provide a key for explaining and, thus, minimising the differences when passing from RDE to MEA.

Based on the information available in the literature (*vide supra*) and since the investigated NOMC electrocatalyst is devoid of metals, the study was performed in an alkaline environment and more specifically with an aqueous 0.1 M KOH solution as electrolyte. The influence of the binder and of the catalyst loading (both at constant binder content and at constant binder-to-catalyst ratio) and of the binder type were systematically evaluated over a wide range of values. Additionally, we studied the effect of using an ink that contains both the binder and the catalyst instead of the

conventional two-step preparation (catalyst and binder added separately). Most of the RDE-studies of doped OMCs or other doped carbons in alkaline environment use Nafion® as binder to attach the electrocatalyst onto the electrode[21,40–47] and, therefore, we chose to employ this ionomer as reference binder. However, Nafion® is a cation-exchange polymer and would thus be unsuitable for application as membrane in a fuel cell operating with an alkaline electrolyte as under these conditions the negatively charged hydroxide ions have to be exchanged between cathode and anode. For this reason, we investigated an anion-exchange polymer (Fumion FAA-3®) as an alternative binder, as this will allow an easier translation of the results of the RDE-study to a fuel cell set-up.

## Results and Discussion

We studied the influence of the ink composition and electrode fabrication method on the ORR activity and selectivity of an NOMC electrocatalyst with high surface area (764 $m^2$ $g^{-1}$) and uniform mesopores (average diameter of 3.3 nm).[2] SEM and TEM images of the synthesised materials evidence a morphology characterised by long tubular carbon structures containing the expected ordered parallel mesopores (Fig. S1). The activity was assessed on the basis of the onset potential, the half-wave potential ($E_{1/2}$) and the kinetic current density ($J_K$) measured with a rotating ring disk electrode in a half-cell setup. The onset potential is not expected to experience major influence from the investigated parameters since in principle it should only depend on the type of active sites present at the surface of the electrocatalyst. The selectivity was assessed based on the number of exchanged electrons ($n$) determined from the slope of the K-L plots and on the amount $H_2O_2$ detected on the Pt ring of the RRDE. In a previous study,[2] we compared this NOMC material to a commercial Pt/C electrocatalyst. At 0.61 V vs. RHE, Pt/C gave a ca. 1.5 times higher kinetic current density and the expected high selectivity towards $H_2O$ ($n$ = 4), whereas the NOMC was more selective towards $H_2O_2$ ($n$ = 2.1). A chronoamperometric test showed that the NOMC material exhibits a much higher stability than the commercial Pt/C electrocatalysts under operating conditions (only 10% decrease in current after 5h).

### Role of the type of ionomer used as binder

The influence on the ORR performance of the type of ionomer that is used to bind the electrocatalyst to the glassy carbon disk of the RDE was investigated here for the first time (Table 1 and Fig. S2, S3). A binder is utilised to grant the adhesion of the catalyst to the RDE at all employed rotation speeds. Ionomers were used as binders as this would facilitate the later application in an actual fuel cell, in which an ionomer is essential to transfer either protons or hydroxide ions between anode and cathode compartments. Currently, Nafion® is the most commonly applied binder in RDE and RRDE studies of electrocatalysts for the

ORR.[4]Even if Nafion® is a proton-conductive polymer, it is often used also for ORR tests in alkaline environments. This has the disadvantage that the obtained results cannot be directly exported for application in a MEA, because an anion-exchange membrane through which hydroxide ions are transferred is required in a fuel cell operating with an alkaline electrolyte, which is the preferred reaction environment for the emerging class of electrocatalysts based on doped carbon materials (as our NOMC). For these reasons, we chose to start our study by investigating the influence on the RDE performance of the binder by comparing the use of Nafion® as binder with that of a hydroxide-conductive polymer (Fumion FAA-3®).While this investigation is important in view of a prospective application in an actual fuel cell, we also aim at finding out if the use of an anion- or a proton-exchange polymer has an influence on the ORR performance at the level of half-cell tests with RDE/RRDE. Additionally, we studied a second proton-conductive polymer as binder, polystyrene sulphonic acid (PSSA). In this case, the purpose was to determine whether this cheaper proton-conductive ionomer could offer a similar performance and thus become an alternative to Nafion®.

**Table 1.** Effect of the binder type on the ORR performance of the NOMC electrocatalyst, at 0.61 V vs. RHE and recorded in an $O_2$-saturated 0.1 M KOH solution with a scan rate of 10 mV $s^{-1}$ at 2500 rpm. $J_K$ was determined based on the geometric surface area of the electrode disk ($A_{geo}$ ≈ 0.20 cm²).

| | *n* | $J_K$ (mA $cm^{-2}$) | Sel. $H_2O_2$ (%) | $E_{onset}$ (V) | $E_{1/2}$ (V) |
|---|---|---|---|---|---|
| Nafion® | 2.2±0.1 | -10.1±0.7 | 92±1 | 0.89 | 0.69 |
| PSSA | 2.2±0.1 | -7.3±0.5 | 92±2 | 0.91 | 0.68 |
| Fumion FAA-3® | 2.0±0.1 | -6.6±0.4 | 100±1 | 0.92 | 0.69 |

As expected, the onset potential did not vary considerably when the ionomer type was changed, though the difference in onset potential betweenFumionFAA-3® and Nafion® seems statistically significant. On the other hand, the selectivity of the ORR shifted towards hydrogen peroxide (higher Sel.$H_2O_2$(%) and *n* closer to two, Table 1) when Fumion FAA-3® was used. This behaviour can be rationalised considering the different nature of the ionomer backbone, which is positively charged in Fumion FAA-3® and negatively in the other two binders. The positive charge can allow a faster removal of hydrogen peroxide, which is present as $HO_2^-$ in an alkaline environment, from the active layer. On the other hand, the negatively charged backbone of Nafion® and PSSA can favour the retention of the $HO_2^-$ ions for a longer time in the catalyst layer due to electrostatic repulsion, thus increasing the probability of further reduction of the peroxide anion to water.

The kinetic current density differed significantly between the three ionomers, with the highest value observed with Nafion®, followed by PSSA and Fumion FAA-3® (Table 1).

We attribute the higher kinetic current density observed with Nafion® compared to Fumion FAA-3® to the higher affinity for water and to the higher oxygen permeability of the former, as indicated by the measured values of water uptake (37 wt.% for Nafion® vs. 26 wt.% for Fumion FAA-3®) and of oxygen permeability (87 Barrer for Nafion® vs. 68 Barrer for Fumion FAA-3®). A higher water uptake implies that more dissolved oxygen can reach the active sites while higher oxygen permeability results in a faster transport of oxygen through the binder layer to the active sites. In turn, this can result in a higher kinetic current density in the RDE tests. However, while higher oxygen permeability can be considered an asset in the RDE setup, the opposite is true in an actual fuel cell, in which oxygen cross-over through the membrane should be avoided as much as possible because it would result in a decrease in the fuel cell efficiency. Therefore, the lower oxygen permeability of Fumion FAA-3® is expected to become an advantage at the MEA stage. Also the ion-conductivity of the ionomers can be used to explain the influence of the binder type on the electrocatalyst performance. A proton-conductivity of 100 mS $cm^{-1}$has been reported for Nafion®,[48] whereas the value reported for PSSA was 70 mS $cm^{-1}$.[49] A hydroxide-conductivity of 50 mS $cm^{-1}$was measured for Fumion FAA-3®.[50] Based on the data available in literature, the higher ion-conductivity for Nafion® is directly related to the higher water uptake.[51,52] Although the trend in ion-conductivity corresponds to that followed by the kinetic current density (Table 1), it should be kept in mind that potassium ions rather than protons are expected to be transported through Nafion® and PSSA in the employed KOH solution.

These results demonstrate that the ionomer does not only play a role as binder but also significantly influences the ORR performance, both in terms of activity and selectivity of the electrocatalyst.

## Influence of the Nafion® loading

Besides the nature of the binder used in the ink, also its loading is expected to have a relevant impact on the electrocatalytic performance. Previous reports on silver nanowires and Pt/C demonstrated that the use of a binder is essential to guarantee the adhesion of the electrocatalyst to the electrode.[13,36] However, it is important that the ionomer loading is not too high, as this is generally detrimental for the ORR performance.[13,36] These findings were confirmed in this study for the NOMC using Nafion® as binder (see Figure 1, S4, S5 and Table 2).

At high rotation speeds (2500 rpm) a high level of noise could be observed in the LSV plots for the electrodes prepared without Nafion® (Fig. 1), which is attributed to the observed detachment of the catalyst from the RRDE. This proves that a binder is necessary for the adhesion of the NOMC electrocatalyst to the electrode. A loading as low as 0.56 µg $cm^{-2}$ is sufficient to efficiently attach the electrocatalyst to the electrode, so that it does not peel off even at high rotation rates. At low loadings, the impact of

Nafion® on the electrocatalytic performance is negligible, as can be seen by comparing the results for Nafion® loadings ≤ 1.11 µg $cm^{-2}$ (Table 2 and Fig. 1 & S4). On the other hand, when the loading of Nafion® is ≥ 2.22 µg $cm^{-2}$, it negatively influences the kinetic current density and the overall current generation (Table 2 and Fig. 1 & S4). It was further observed that Nafion® loadings above 2.22 µg $cm^{-2}$ resulted in decreased selectivity towards hydrogen peroxide (*n* increases, Sel.$H_2O_2$(%) decreases, see Table 2). This is attributed to the longer residence time (i.e. longer diffusion path) of the formed species as the Nafion® layer becomes thicker and more extensive: the longer the $HO_2^-$ ions are retained in the catalytically active layer, the more likely becomes their further reduction. As the values of the selectivity determined with the K-L equations and those based on the ring currents agree well with each other, and since the same electrocatalyst is used in all tests, the observed decreases in kinetic current density can only be attributed to lower accessibility of the active sites as a consequence of gradual pore blocking and/or of a longer diffusion path caused by the increased Nafion® content.

The onset potential does not differ significantly as a function of the Nafion® loading and this means that the trend in the half-wave potential is connected to that of the kinetic current density (Table 2). For the electrodes prepared without Nafion®, the values for the different parameters could not be determined because of the noise. Finally, a Nafion® loading of 44.4 µg $cm^{-2}$ was too high to generate any current. Most likely, the Nafion® layer completely blocked the access of $O_2$ to the active sites of NOMC.

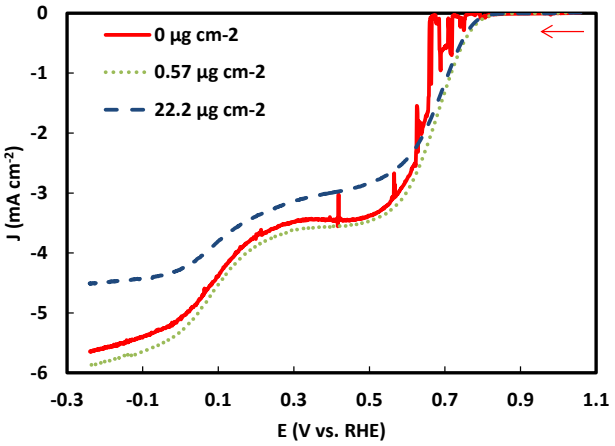


**Figure 1.** Impact of Nafion® loading on the electrocatalytic performance of NOMC, measured on a RRDE in an $O_2$-saturated 0.1 M KOH solution with a scan rate of 10 mV $s^{-1}$ at 2500 rpm. The red arrow indicates the scan direction. J was determined based on the geometric surface area of the disk ($A_{geo}$ ≈ 0.20 $cm^2$).

**Table 2.** Influence of Nafion® loading on the ORR performance of the NOMC electrocatalyst, at 0.61 V vs. RHE and recorded in an $O_2$-saturated 0.1 M KOH solution with a scan rate of 10 mV $s^{-1}$ at 2500 rpm. $J_K$ was determined based on the geometric surface area of the disk ($A_{geo}$ ≈ 0.20 $cm^2$).

| Nafion loading (µg $cm^{-2}$) | *n* | $J_K$ (mA $cm^{-2}$) | Sel. $H_2O_2$ (%) | $E_{onset}$ (V) | $E_{1/2}$ (V) |
|---|---|---|---|---|---|
| 0 | / | / | / | / | / |
| 0.56 | 2.2±0.1 | -9.9±0.2 | 91±1 | 0.89 | 0.68 |
| 1.11 | 2.2±0.1 | -10.1±0.3 | 92±1 | 0.89 | 0.69 |
| 2.22 | 2.5±0.2 | -4.6±0.5 | 74±2 | 0.89 | 0.65 |
| 22.2 | 2.7±0.1 | -4.8±0.3 | 65±1 | 0.90 | 0.66 |
| 44.4 | / | / | / | / | / |

## Influence of the electrocatalyst loading

The impact of the electrocatalyst loading on the ORR performance was investigated to determine which reduction

mechanism, i.e. the direct four electron reduction or the stepwise two electron reduction with hydrogen peroxide as an intermediate, is the dominant one over the NOMC. A previous study on porous electrocatalysts showed that the number of exchanged electrons should not differ in function of the electrocatalyst loading if the four electron reduction mechanism is followed.[35] Since the selectivity towards water increases at higher catalyst loadings (*n* closer to 4 and lower Sel.$H_2O_2$(%), see Table 3 and Fig. S7), it is concluded that the path involving hydrogen peroxide as an intermediate is predominant in the ORR catalysed by our NOMC in basic medium. This is a consequence of the longer residence time of reagent and products in the active layer, which leads to a higher probability of the formed peroxide to encounter another active site and to get reduced further to $H_2O$ prior to being released. The overall current also increases with the electrocatalyst loading (Figure 2 and S6 to S8). The same trend is followed by the kinetic current density (up to 100 µg $cm^{-2}$, see Table 3). This increase is not only due to the higher number of active sites that is available at higher loadings, but also to the observed increase in number of exchanged electrons at higher electrocatalyst loading ($J_K$ is proportional to *n*). If the magnitude of the current density is plotted as a function of the catalysts loading (Fig. 3), the first increase in electrocatalyst loading (from 10 to 22 µg $cm^{-2}$) leads to the expected increase in $J_K$ (assuming proportionality to both catalyst loading and *n*), while this is not the case if the electrocatalyst loading is further increased. This trend suggests that up to a loading of 22 µg $cm^{-2}$ the porosity of the NOMC grants unrestrained access to its active sites. At higher loadings the reaction rate may become limited by the longer time necessary to transport $O_2$through the pores to the inner active sites, i.e. those located furthest away from the surface. Pores blockage is also more likely to occur at higher catalyst loading. It should be noted that the observed trends in selectivity and activity as a function of the electrocatalyst loading are specific of the texture of the NOMC material and that electrocatalysts displaying a different pores size and structure or non-porous ones are expected to behave differently (e.g. in the absence of a pore system, even the first increase in the electrocatalyst loading is not expected to lead to a proportional increase in current density). For the above statements to be strictly correct, it is necessary that the GC disk is at least covered with a monolayer of the electrocatalyst, otherwise the GC disk can also contribute to the activity. To verify this, an optical microscope was used to visualise the surface coverage of the GC disks (see Fig. S9). Only for the lowest catalyst loading (10 µg $cm^{-2}$), a significant fraction of the GC disk (40 to 50%) remains uncovered, which indicates that the results of the loading in question have to be considered with caution. To get further insight into the influence of the GC disk on the overall ORR performance, RRDE measurements were performed with a pure GC disk (see Fig. S7): the overpotential towards the ORR is higher than with NOMC and the results of the Koutécky-Levich

analysis at 0.61 V reveal that *n* is 0.7 and $J_K$ is 2.8 mA $cm^{-2}$. This means that the influence of the exposed GC disk on the results of the 10 µg $cm^{-2}$ loading is minor, though it cannot be completely disregarded.

**Table 3.** Influence of the electrocatalyst loading on the ORR performance of NOMC at constant Nafion® loading of 1.11 µg $cm^{-2}$, at 0.61 V vs. RHE and recorded in an $O_2$-saturated 0.1 M KOH solution with a scan rate of 10 mV $s^{-1}$ at 2500 rpm. $J_K$ was determined based on the geometric surface area of the disk ($A_{geo}$ ≈ 0.20 $cm^2$).

| NOMC loading (µg $cm^{-2}$) | *n* | $J_K$ (mA $cm^{-2}$) | Sel. $H_2O_2$ (%) | $E_{onset}$ (V) | $E_{1/2}$ (V) |
|---|---|---|---|---|---|
| 10 | 2.0±0.1 | -3.8±0.2 | 99±1 | 0.90 | 0.65 |
| 22 | 2.2±0.1 | -9.9±0.5 | 92±1 | 0.90 | 0.70 |
| 25 | 2.2±0.1 | -10.1±0.3 | 92±1 | 0.89 | 0.69 |
| 50 | 2.6±0.2 | -11.5±0.6 | 73±2 | 0.91 | 0.72 |
| 100 | 2.7±0.2 | -13.7±1.2 | 67±2 | 0.90 | 0.72 |
| 1000 | 2.3±0.4 | -6.4±0.5 | 85±5 | 0.90 | 0.65 |

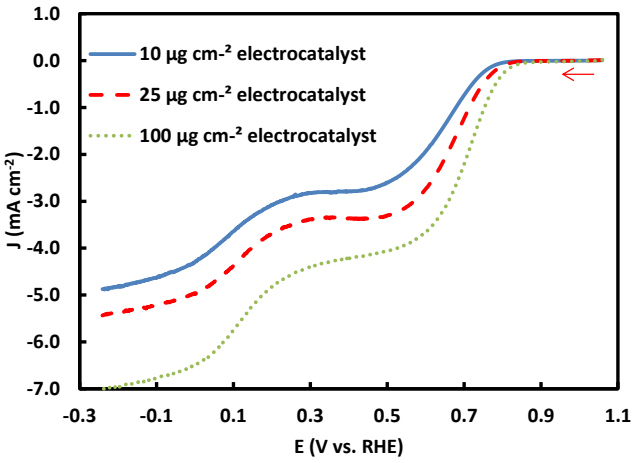


**Figure 2.** Impact of catalyst loading on the electrocatalytic performance of NOMC, recorded on a RRDE in an $O_2$-saturated 0.1 M KOH solution with a scan rate of 10 mV $s^{-1}$ at 2500 rpm and at constant Nafion® loading (1.11 µg $cm^{-2}$). The red arrow indicates the scan direction. J was determined based on the geometric surface area of the disk ($A_{geo}$ ≈ 0.20 $cm^2$).

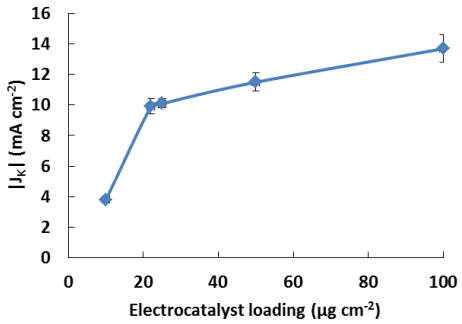


**Figure 3.** Kinetic current density as a function of electrocatalyst loading. $J_K$ was determined based on the geometric surface area of the disk ($A_{geo}$ ≈ 0.20 $cm^2$).

Finally, since the type of active site did not differ when modifying the electrocatalyst loading, the onset potential did not change significantly either. Therefore, the trend in half-wave potential follows that of the kinetic current density. For the electrocatalyst loading of 1000 µg $cm^{-2}$, a decrease in *n* and $J_K$ was observed. This was caused by the detachment of the electrocatalyst from the RRDE, which was visually observed at high rotation rates (> 2000 rpm). The Nafion® content was thus not sufficiently high to bind all the active material on the electrode at these rotation rates. This result stimulated us to explore the influence of the electrocatalyst loading on the ORR performance at constant electrocatalyst-to-Nafion® ratio (see Table 4 and figure S10 and S11).

**Table 4.** Influence of the electrocatalyst loading on the ORR performance at constant electrocatalyst-to-Nafion® mass ratio of 22.5, at 0.61 V vs. RHE and recorded in an $O_2$-saturated 0.1 M KOH solution with a scan rate of 10 mV $s^{-1}$ at 2500 rpm. $J_K$ was determined based on the geometric surface area of the disk ($A_{geo}$ ≈ 0.20 $cm^2$).

| NOMC loading (µg $cm^{-2}$) | *n* | $J_K$ (mA $cm^{-2}$) | Sel. $H_2O_2$ (%) | $E_{onset}$ (V) | $E_{1/2}$ (V) |
|---|---|---|---|---|---|
| 10 | 2.1±0.1 | -7.7±0.4 | 95±1 | 0.90 | 0.67 |
| 25 | 2.2±0.1 | -10.1±0.3 | 92±1 | 0.89 | 0.69 |
| 50 | 2.7±0.2 | -10.0±0.6 | 65±2 | 0.91 | 0.73 |
| 100 | 3.2±0.3 | -10.3±0.3 | 40±4 | 0.91 | 0.73 |

The trends observed by increasing the catalyst loading at constant electrocatalyst-to-Nafion® ratio are similar to those observed with fixed Nafion® amount: the selectivity to water increases (*n* increases and Sel.$H_2O_2$(%) decreases) whereas the onset potential does not differ significantly. However, the kinetic current density does not tend to increase with *n*, which was the case at constant Nafion® loading. This is a consequence of the negative impact of the increased Nafion® loading on the accessibility of the active site (*vide supra*), which negatively influences the reaction rate (*vide supra*).

## Stepwise vs. simultaneous preparation

Finally, it was investigated whether the electrocatalytic performance benefits from a separate addition of catalyst and Nafion® or if the same results can be obtained with a simultaneous addition without modifying the final electrode composition. This one-step approach has been scarcely employed so far,[53] but is more straightforward and may thus represent an attractive alternative to the currently dominant two-step procedure. The results in Table 5 show no clear difference between the two methods (see also Fig. S12and S13). This means that the standard procedure for the preparation of the electrode can be simplified by adding electrocatalyst and Nafion® simultaneously. This decrease in the number of experimental variables is also expected to lead to an increased reproducibility of the LSV tests.

**Table 5.** Comparison of performance in ORR between the stepwise and the simultaneous addition of Nafion® and electrocatalyst, recorded on a RRDE in an $O_2$-saturated 0.1 M KOH solution with a scan rate of 10 mV $s^{-1}$ at 2500 rpm. $J_K$ was determined based on the geometric surface area of the disk ($A_{geo}$ ≈ 0.20 $cm^2$).

| Method | *n* | $J_K$ (mA $cm^{-2}$) | Sel. $H_2O_2$ (%) | $E_{onset}$ (V) | $E_{1/2}$ (V) |
|---|---|---|---|---|---|
| Stepwise | 2.2±0.1 | -10.1±0.3 | 92±1 | 0.89 | 0.69 |
| Simultaneous | 2.2±0.1 | -10.1±0.2 | 93±1 | 0.90 | 0.70 |

## Conclusions

The impact of the composition and preparation of the electrocatalyst layer on the rotating-disk electrode used in the evaluation of the ORR performance of an N-doped ordered mesoporous carbon electrocatalyst in 0.1 M KOH as electrolyte was investigated here for the first time. In agreement with literature reports on other porous electrocatalysts, an increase in the electrocatalyst loading resulted in a higher electron transfer number. By varying the type and loading of binder, it was concluded that the ORR performance is also influenced by the nature and amount of ionomer. The influence of the binder type had never been investigated thus far for any type of electrocatalyst. It was determined that the selectivity towards water in an alkaline environment decreases when an anionomer as Fumion FAA-3® is used as binder instead of a proton-exchange polymer. Furthermore, a correlation was found between the observed current density and the water uptake, the oxygen permeability and ion-conductivity of the ionomer. The impact of the binder loading was studied with Nafion® and showed an increase in selectivity and a decrease in kinetic current density at higher binder loadings. This agrees well

with the results that have been reported with an anion-exchange polymer from Tokuyama (ionomer AS-4) used as binder for a silver nanowire electrocatalyst.[13] Finally, it was determined that the time and cost efficiency of the electrode fabrication process could be improved by simultaneously adding the catalyst and the binder to the electrode. These trends have been obtained using an NOMC as electrocatalyst but are expected to be valid also for other electrocatalysts having a similar ordered mesoporous structure.

Based on the above trends it is possible to determine an optimal composition of the NOMC electrocatalyst layer both for the cogeneration of hydrogen peroxide and electricity and for the case when the sole purpose is electricity generation. For the former, FumionFAA 3® should be used as ionomer, applying as low loadings as possible (*e.g.* 0.57 µg $cm^{-2}$) to avoid the negative effects on the current density and the selectivity. With respect to the catalyst, a lower loading also ensures a higher selectivity towards $H_2O_2$. On the other hand, for generating water the optimal composition of the electrocatalyst layer would be 100 µg $cm^{-2}$ of NOMC and 4.44 µg $cm^{-2}$ of Nafion®. Higher Nafion® loadings would have a negative impact on the current density, although possibly further increasing the selectivity. This relatively high loading is needed to increase the selectivity, though it also decreases the efficiency of the catalyst due to decreased accessibility of the active sites.

This systematic study allowed establishing the relevance and the extent of the influence of the ink composition and electrode fabrication method on the ORR performance of a metal-free NOMC electrocatalyst: the values for $J_k$ varied between -3.8 and -13.7 mA $cm^{-2}$ and those of *n* between 2.0 and 3.2, simply by changing the composition of the electrocatalyst layer. This study thus clearly underlines the need of taking these parameters into account when comparing different electrocatalysts. This important conclusion is not limited to NOMCs but is of general validity, though the effect of each parameter could vary for different electrocatalysts. In this context, it would be advised to define a standard composition of the electrocatalyst layer to be used in RDE studies of novel electrocatalysts. Only in this way it would become possible to compare in a meaningful way the performance of novel electrocatalysts reported by different research groups. This comparison is currently severely hampered by the wide variety in electrode compositions and preparation methods employed in different studies. Based on our results, we propose to use a Fumion FAA-3® loading of 0.56 µg $cm^{-2}$, an electrocatalyst loading of 25 µg $cm^{-2}$ and the simultaneous addition of binder and catalyst as standard composition and preparation method of the electrocatalyst layer in the RDE-investigation of the oxygen reduction reaction in alkaline environment. The catalyst and binder loadings were kept low to limit the influence of the thickness of the active layer on the outcome of the ORR

tests. We plead for using an anion-exchange polymer as binder, as this would offer an evaluation of the electrocatalytic performance in alkaline environment with as underlying idea to decide on its applicability in actual fuel cell technology. In this context, we believe that the use of Nafion® as binder in RDE-studies in alkaline environment should be discouraged, as this cation-exchange polymer would be unsuitable for use as membrane in an alkaline fuel cell.

In future perspective, the results of this systematic study can also have important implications in understanding and, therefore, minimising the differences in the ranking of electrocatalysts that are often observed when passing from RDE-results to application in MEAs used in fuel cells.

## Experimental Section

### Synthesis of the electrocatalyst

A detailed description of the synthesis method of the NOMC electrocatalyst has been reported elsewhere.[2] A brief summary is given here. First, the SBA-15 mesoporous silica used as hard template was synthesised, calcined and impregnated with aniline. After polymerisation, the material was subjected to a first pyrolysis step for 3h at 900°C and the remaining pore volume was filled up with dihydroxynaphthalene, followed by a second pyrolysis step for 5h at 900°C. In a final step, the template was etched away by treatment with a 2.5 wt% solution of NaOH in $EtOH/H_2O$ to obtain the N-doped ordered mesoporous carbon material that was used as electrocatalyst in this study.

### Electrochemical study

The electrocatalytic performance of the NOMC in the oxygen reduction reaction as a function of the composition and fabrication method of the electrocatalyst layer was evaluated by means of linear sweep voltammetry (LSV) carried out with a rotating ring disk electrode (RRDE). LSV measurements were conducted at various rotation speeds (400-2500 rpm). The experiments were carried out at room temperature in a conventional three-electrode cell from Gamry with a modulated speed rotator of Pine and a rotating ring disk electrode connected to a Gamry Interface 1000 bipotentiostat. An Ag/AgCl (saturated KCl, E° = 0.197 V vs. SHE) reference electrode was used in combination with a Pt gauze counter electrode, the latter being located in a separate compartment connected to the rest of the cell through a frit (see Fig. S14).The internal salt bridge of the reference electrode was filled with 0.1 M aqueous KOH. A glassy carbon, replaceable disk with a surface area of 0.196 $cm^2$ was employed as inert carrier for the working electrode. A Pt ring was used to detect and quantify the hydrogen peroxide that is produced during the ORR. The ORR was performed in an aqueous 0.1M KOH electrolyte, which was previously saturated with $O_2$ by bubbling $O_2$ gas into the solution for 30 min. Afterwards, $O_2$ saturation was maintained by a flow of $O_2$ just above the electrolyte during the whole voltammetry experiment. The potential of the disk

was varied from 0.1 to -1.2 V vs. Ag/AgCl at a potential sweep rate of 10 $mVs^{-1}$. The Pt-ring potential was kept constant at 0.5 V, which is positive enough to reoxidise all the produced hydrogen peroxide back to oxygen. The ring currents are thus an indication for the hydrogen peroxide production. All potentials were referred to the reversible hydrogen electrode (RHE) according to the following equation (Eq. 3)[54]:

E (RHE) = E (Ag/AgCl (Sat. KCl) + 0.197 V + 0.059 pH (3)

The current densities were calculated based on the geometric surface area of the glassy carbon electrode as the actual surface area cannot be determined accurately. The actual surface area is a function of the specific surface area of the electrocatalyst, and of the amounts of electrocatalyst and of binder that are deposited on the disk. This implies that the obtained values of kinetic current density include contributions of both the intrinsic activity (per surface unit) and of the surface area of the electrocatalyst.[55] This allows a meaningful ranking of the performance of different electrocatalytic materials. It should be noted that this is conceptually different from reports in which the kinetic current density is normalised through the electrochemically active surface area (EASA), in which case only the intrinsic activity (per surface unit) is evaluated.

The standard electrocatalyst ink was prepared by suspending 2 mg of electrocatalyst in 1.5 ml of a 1:1 volume mixture of isopropanol and water. This mixture of solvents was chosen since a previous study demonstrated that this composition leads to the most stable suspensions (up to days without settling).[56] The ink was sonicated for 1 h, under which conditions a homogeneous suspension was obtained. 3.47 µL ± 0.04 µL of electrocatalyst ink was then deposited with a pipette (Finnpipette F1, 0.5-5 µl) onto the disk surface, yielding an approximate catalyst loading of 25 µg $cm^{-2}$. After drying, a thin Nafion® film was applied by depositing 4.86 µl ± 0.04 µL of a 0.05 wt% Nafion® solution in 50/50 vol% isopropanol/water (Sigma Aldrich) with the same type of pipette, followed by a final drying step at room temperature giving an approximate Nafion® loading of 1.11 µg $cm^{-2}$. Based on this procedure, the binder will tend to be present as a layer covering the electrocatalyst layer.

The standard procedure described above was modified in different ways to investigate the influence of various parameters on the ORR performance. First of all, the influence of the binder type was studied by employing either polystyrene sulphonic acid (PSSA, Sigma Aldrich) or Fumion FAA-3® ionomer (a commercially available fluorocarbon polymer with quaternary ammonium groups providing the anion exchange function, supplied by Fumatech GmbH) instead of Nafion® (with a loading of 1.11 µg $cm^{-2}$in all cases). Next, the influence of the binder (Nafion®) loading on the performance was investigated by applying Nafion® loadings in a range from 0 to 44.4 µg $cm^{-2}$. The effect of the catalyst loading was also investigated by varying the final loading from 10 to 1000 µg $cm^{-2}$,either at a

constant Nafion® loading (1.11 μg $cm^{-2}$) or at a constant electrocatalyst-to-Nafion® mass ratio (22.5). In all these studies, the different loadings were achieved by depositing different volumes of the standard electrocatalyst suspension and binder solution described above. A final variation to this standard method was made by adding both Nafion® and electrocatalyst to the same ink and adding them to the glassy carbon disk at the same time without modifying the final electrode composition.

The LSV measurements allowed to calculate the onset potential, the half-wave potential ($E_{1/2}$), the kinetic current density ($J_K$) and the number of exchanged electrons (*n*). The onset potential was determined as the potential at which the current density exceeds 10μA $cm^{-2}$ in the LSV plots. The half-wave potential was determined as the potential at which the first derivative of the LSV plots with respect to the potential reaches a maximum. The kinetic current density and the number of exchanged electrons were determined based on the Koutécky-Levich (K-L) equations (4-6):

$$\frac{1}{J} = \frac{1}{J_K} + \frac{1}{J_D} = \frac{1}{J_K} + \frac{1}{B\omega^{1/2}} \quad (4)$$

where J is the measured current density, which can be expressed in terms of kinetic current density ($J_K$) and diffusion-limited current density ($J_D$). ω Is the angular velocity of the RRDE. B and $J_K$ are defined as follows:

$$B = 0.62nFC_0(D_0)^{2/3}\nu^{-1/6} \quad (5)$$

$$J_K = nFkC_0 \quad (6)$$

where F is the Faraday constant (96485 C $mol^{-1}$), *n* is the number of exchanged electrons, *k* is the electron transfer rate constant (at a given potential), $C_0$ is the bulk $O_2$ concentration (1.2 x $10^{-6}$mol $cm^{-3}$), ν is the kinematic viscosity of the electrolyte (0.01 $cm^2$ $s^{-1}$) and $D_0$ is the diffusion coefficient of $O_2$ (1.9 x $10^{-5}$ $cm^2$ $s^{-1}$) [2]. The kinetic current density can be determined from the intercept of the K-L plots, whereas the value of *n*, which provides an indication of the selectivity, can be determined from the slope of the K-L plots.

It is noteworthy to mention that the Koutécky-Levich equations were derived for flat surface electrodes, in which the geometric surface area of the electrode is equal to the actual active surface area. This is not the case for porous electrocatalysts, for which the actual surface area is typically much larger than the geometric surface area of the electrode (*vide supra*).[28] In this context, it should be taken into account that the kinetic current density obtained using the K-L equations is measured with respect to the geometric surface area of the electrode also when analysing porous electrocatalysts. As a consequence, the value of kinetic current density can change as a function of the loading of the porous electrocatalyst, because a higher loading can lead to a larger accessible surface area (if the pores remain accessible) and, therefore, to a higher number of active sites.[57,58]

It should also be noted that the porous structure of the electrocatalyst could in principle lead to diffusion

limitations, particularly if the pores were partially obstructed (e.g. by using different amounts of binder). In such case, the value of the diffusion coefficient ($D_0$) would change and the expression of B would not allow anymore calculating the value of *n* correctly. Therefore, we estimated the selectivity first of all on the basis of the amount of $H_2O_2$ that is detected on the Pt ring (Sel. $H_2O_2$). This reliable value was then compared to the values of *n* that are determined with the K-L equations. Since the obtained values fully agree with each other, we can conclude that no diffusion limitation is affecting the tests. Sel. $H_2O_2$ is determined using the following equation:

$$\text{Sel.}H_2O_2(\%) = \frac{200 \times I_{ring}}{(N \times I_{disk}) + I_{ring}} \quad (7)$$

where $I_{ring}$ and $I_{disk}$ are the currents collected on the Pt ring and on the catalyst-coated disk, respectively. N is the collection efficiency and was determined to be in the interval of 0.19 to 0.25 for our RRDE system (depending on the loading of electrocatalyst and binder) by using the $Fc/Fc^+$ redox couple. These measurements were performed at 1600 rpm and at a ring potential of 0.8 V vs. Ag/AgCl. The importance of determining the collection efficiency for each loading at the employed rotation of the RRDE is in line with the findings of a recent report investigating the correlation between these experimental parameters.[59] Equation (7) is valid under the assumption that only $H_2O_2$ and $H_2O$ are produced from the oxygen reduction.

The values of *n*, $J_K$ and Sel.$H_2O_2$(%) were all determined at 0.61 V vs. RHE, as this potential corresponds to the mixed kinetic-diffusion regime.[60,61] The mixed kinetic-diffusion regime is generally chosen as it is the only region where the $J_K$ and $J_D$ can accurately be determined. At more positive potentials (> 0.71 V vs. RHE), $J_D$ is so small that a minor fluctuation in $J_D$ will have an enormous impact on the value of $J_K$ (as the inverse of a small value gives a large number). At more negative potentials, $J_K$ becomes so large that $1/J_K$ approaches zero and $J_K$ can no longer be determined.[28]

All measurements were performed in duplicate (or in triplicate if the deviation between the first two measurements was large) and the average values and standard deviations are reported. For the onset potential and the half-wave potential the standard deviation was never larger than 0.01 V and is therefore not reported in the rest of the paper.

The water uptake of Nafion® and Fumion FAA-3® were determined by immersing a sample (3 x 3 cm) that was cut from a commercial membrane (186 μm for Nafion® and 30 μm thickness Fumion FAA-3®) in a 250 ml beaker containing 125 ml of boiling water.

$$\text{Water uptake} = \frac{m_{wet} - m_{dry}}{m_{dry}} \ 100\% \quad (8)$$

where $m_{dry}$ is the mass of the membrane sample after drying at 50°C in a vacuum oven overnight and $m_{wet}$ is the mass of the membrane sample after equilibration for 1 h in boiling water at 100°C.

A High-Throughput Gas Separator (HTGS) system was used to measure the $O_2$ permeability of the membranes. This system enables the quasi parallel measurement of 16 membrane coupons with an effective permeation surface of 1.54 cm². Prior to the measurement, the membranes were dried in a vacuum oven at 60°C overnight. The permeability was measured by directing the permeating $O_2$ gas flow to a MKS Baratron pressure transducer (with a volume of 50 cm³) which registers pressure in function of time. An $O_2$ feed pressure of 5 bar was applied. After steady state, the linear dependence between pressure and time (dP/dt) was used in the following expression to calculate the permeability:

$$\text{Permeability (Barrer)} = 10^{10}\frac{dP}{dt}\frac{LV}{10000000\ A\ \Delta P\ TR} \quad (9)$$

where ΔP is the pressure over the membrane (bar), A is the membrane surface (cm²), L is the membrane thickness (L = 183 µm for the commercial Nafion® membrane and L = 30 µm for the Fumion FAA-3® membrane), V is the volume of the pressure transducer (cm³), T is the temperature(K) and R the gas constant (0.278 $cm^3 \cdot cmHg \cdot cm^{-3}_{(STP)} \cdot K^{-1}$).

## Acknowledgements

The authors acknowledge sponsoring from Flemish agency for Innovation by Science and Technology (IWT) in the frame of a Ph.D. grant (ND). We thank Jeroen Didden for his help with the oxygen permeability measurements.

**Keywords:** N-doped ordered mesoporous carbon, selectivity, activity, rotating disk electrode composition, oxygen reduction reaction

[1] S. Srinivasan, *Fuel Cells: From Fundamentals to Applications*, **2006**.
[2] X. Sheng, N. Daems, B. Geboes, M. Kurttepeli, S. Bals, T. Breugelmans, A. Hubin, I. F. J. Vankelecom, P. P. Pescarmona, *Appl. Catal. B Environ.* **2015**, *176–177*, 212–224.
[3] H. A. Gasteiger, S. S. Kocha, B. Sompalli, F. T. Wagner, *Appl. Catal. B Environ.* **2005**, *56*, 9–35.
[4] N. Daems, X. Sheng, I. F. J. Vankelecom, P. P. Pescarmona, *J. Mater. Chem. A* **2014**, *2*, 4085–4110.
[5] M. Schulze, N. Wagner, T. Kaz, K. A. Friedrich, *Electrochim. Acta* **2007**, *52*, 2328–2336.
[6] C. Su, T. Yang, W. Zhou, W. Wang, X. Xu, Z. Shao, *J. Mater. Chem. A Mater. energy Sustain.* **2016**, *4*, 4516–4524.
[7] Y. Zhu, C. Su, X. Xu, W. Zhou, R. Ran, Z. Shao, *Chem. - A Eur. J.* **2014**, *20*, 13533–13542.
[8] C. Zhang, W. Zhang, S. Yu, D. Wang, W. Zhang, W. Zheng, M. Wen, H. Tian, K. Huang, S. Feng, et al., *ChemElectroChem* **2017**, *4*, 1268.
[9] G. Wu, K. L. More, C. M. Johnston, P. Zelenay, *Science* **2011**, *332*, 443–447.
[10] T.-P. Fellinger, F. Hasché, P. Strasser, M. Antonietti, *J. Am. Chem. Soc.* **2012**, 4072–4075.
[11] D.-W. Wang, D. Su, *Energy Environ. Sci.* **2014**, *7*, 576.
[12] L. Wang, L. Zhang, J. Zhang, *Electrochem. commun.* **2011**, *13*, 447–449.
[13] A. J. Lemke, A. W. O'Toole, R. S. Phillips, E. T. Eisenbraun, *J. Power Sources* **2014**, *256*, 319–323.
[14] S. J. Hamrock, M. a. Yandrasits, *J. Macromol. Sci. Part C* **2006**, *46*, 219–244.
[15] J. Healy, C. Hayden, T. Xie, K. Olson, R. Waldo, M. Brundage, H. Gasteiger, J. Abbott, *Fuel Cells* **2005**, *5*, 302–308.
[16] A. Bonakdarpour, C. Delacote, R. Yang, A. Wieckowski, J. R. Dahn, *Electrochem. commun.* **2008**, *10*, 611–615.
[17] A. Bonakdarpour, M. Lefevre, R. Yang, F. Jaouen, T. Dahn, J.-P. Dodelet, J. R. Dahn, *Electrochem. Solid-State Lett.* **2008**, *11*, B105.
[18] T. Xing, J. Sunarso, W. Yang, Y. Yin, A. M. Glushenkov, L. H. Li, P. C. Howlett, Y. Chen, *Nanoscale* **2013**, *5*, 7970–6.
[19] University of York, "Hydrogen Peroxide," **2014**.
[20] C. W. Jones, H. J. Clark, in *Appl. Hydrog. Peroxide Deriv. RSC, UK*, **1999**, pp. 1–36.
[21] R. Liu, D. Wu, X. Feng, K. Müllen, *Angew. Chemie - Int. Ed.* **2010**, *49*, 2565–2569.
[22] N. Ramaswamy, S. Mukerjee, *J. Phys. Chem. C* **2011**, *115*, 18015–18026.
[23] N. Ramaswamy, S. Mukerjee, *Adv. Phys. Chem.* **2012**, *2012*, 17.
[24] Q. Li, R. Cao, J. Cho, G. Wu, *Adv. Energy Mater.* **2014**, *4*, 1301415–1301434.
[25] Z. Yang, H. Nie, X. Chen, X. Chen, S. Huang, *J. Power Sources* **2013**, *236*, 238–249.
[26] J. P. Paraknowitsch, A. Thomas, *Energy Environ. Sci.* **2013**, *6*, 2839–2855.

[27] F. Jaouen, E. Proietti, M. Lefèvre, R. Chenitz, J.-P. Dodelet, G. Wu, H. T. Chung, C. M. Johnston, P. Zelenay, *Energy Environ. Sci.* **2011**, *4*, 114–130.

[28] A. J. Bard, L. R. Faulkner, *Electrochemical Methods : Fundamentals and Applications*, Wiley, **2001**.

[29] E. J. Biddinger, D. Von Deak, D. Singh, H. Marsh, B. Tan, D. S. Knapke, U. S. Ozkan, *J. Electrochem. Soc.* **2011**, *158*, B402.

[30] W. Jin, H. Du, S. Zheng, H. Xu, Y. Zhang, *J. Phys. Chem. B* **2010**, *114*, 6542–6548.

[31] I. Takahashi, S. S. Kocha, *J. Power Sources* **2010**, *195*, 6312–6322.

[32] D. Shin, B. Jeong, M. Choun, J. D. Ocon, J. Lee, *RSC Adv.* **2015**, *5*, 1571–1580.

[33] S. S. Kocha, J. W. Zack, S. M. Alia, K. C. Neyerlin, B. S. Pivovar, *ECS Trans.* **2012**, *50*, 1475–1485.

[34] D. Geng, N. Ding, T. S. A. Hor, Z. Liu, X. Sun, Y. Zong, *J. Mater. Chem. A* **2015**, *3*, 1795–1810.

[35] F. Jaouen, J. P. Dodelet, *J. Phys. Chem. C* **2009**, *113*, 15422–15432.

[36] J. M. Song, S. Y. Cha, W. M. Lee, *J. Power Sources* **2001**, *94*, 78–84.

[37] D. G. Lee, O. Gwon, H. S. Park, S. H. Kim, J. Yang, S. K. Kwak, G. Kim, H. K. Song, *Angew. Chemie - Int. Ed.* **2015**, *54*, 15730–15733.

[38] K. J. J. Mayrhofer, D. Strmcnik, B. B. Blizanac, V. Stamenkovic, M. Arenz, N. M. Markovic, *Electrochim. Acta* **2008**, *53*, 3181–3188.

[39] M. Shao, *Electrocatalysis in Fuel Cells, a Non- and Low-Platinum Approach*, Springer, **2013**.

[40] D. S. Yang, D. Bhattacharjya, M. Y. Song, F. Razmjooei, J. Ko, Q. H. Yang, J. S. Yu, *ChemCatChem* **2015**, *7*, 2882–2890.

[41] D. S. Yang, D. Bhattacharjya, M. Y. Song, J. S. Yu, *Carbon N. Y.* **2014**, *67*, 736–743.

[42] N. Gavrilov, I. a. Pašti, M. Mitrić, J. Travas-Sejdić, G. Ćirić-Marjanović, S. V. Mentus, *J. Power Sources* **2012**, *220*, 306–316.

[43] Z. Yang, J. Wu, X. Zheng, Z. Wang, R. Yang, *J. Power Sources* **2015**, *277*, 161–168.

[44] J. Y. Cheon, J. H. Kim, J. H. Kim, K. C. Goddeti, J. Y. Park, S. H. Joo, *J. Am. Chem. Soc.* **2014**, *136*, 8875–8878.

[45] H. Wang, X. Bo, Y. Zhang, L. Guo, *Electrochim. Acta* **2013**, *108*, 404–411.

[46] C. Han, X. Bo, Y. Zhang, M. Li, L. Guo, *J. Power Sources* **2014**, *272*, 267–276.

[47] W. Yang, T. P. Fellinger, M. Antonietti, *J. Am. Chem. Soc.* **2011**, *133*, 206–209.

[48] "Properties of Nafion ® PFSA Membrane," **n.d.**

[49] C. S. Fadley, R. A. Wallace, *J. Electrochem. Soc.* **1968**, *115*, 1264–1270.

[50] B. Britton, S. Holdcroft, *J. Electrochem. Soc.* **2016**, *163*, F353–F358.

[51] M. Eikerling, A. A. Kornyshev, A. M. Kuznetsov, J. Ulstrup, S. Walbran, *J. Phys. Chem. B* **2002**, *105*, 3646–3662.

[52] T. P. Pandey, A. M. Maes, H. N. Sarode, B. D. Peters, S. Lavina, K. Vezzù, Y. Yang, S. D. Poynton, J. R. Varcoe, S. Seifert, et al., *Phys. Chem. Chem. Phys.* **2015**, *17*, 4367–4378.

[53] G. Chen, J. Sunarso, Y. Zhu, J. Yu, Y. Zhong, W. Zhou, Z. Shao, *ChemElectroChem* **2016**, *3*, 1760–1767.

[54] J. Yu, G. Chen, J. Sunarso, Y. Zhu, R. Ran, Z. Zhu, W. Zhou, Z. Shao, *Adv. Sci.* **2016**, *3*, 1–8.

[55] X. Sheng, B. Wouters, T. Breugelmans, A. Hubin, I. F. J. Vankelecom, P. P. Pescarmona, *Appl. Catal. B Environ.* **2014**, *147*, 330–339.

[56] B. Geboes, I. Mintsouli, B. Wouters, J. Georgieva, A. Kakaroglou, S. Sotiropoulos, E. Valova, S. Armyanov, A. Hubin, T. Breugelmans, *Appl. Catal. B Environ.* **2014**, *150–151*, 249–256.

[57] J. Masa, C. Batchelor-McAuley, W. Schuhmann, R. G. Compton, *Nano Res.* **2014**, *7*, 71–78.

[58] C. Batchelor-Mcauley, R. G. Compton, *J. Phys. Chem. C* **2014**, *118*, 30034–30038.

[59] R. Zhou, Y. Zheng, M. Jaroniec, S.-Z. Qiao, *ACS Catal.* **2016**, *6*, 4720–4728.

[60] U. a. Paulus, T. J. Schmidt, H. a. Gasteiger, R. J. Behm, *J. Electroanal. Chem.* **2001**, *495*, 134–145.

[61] B. Wouters, X. Sheng, A. Boschin, T. Breugelman, E. Ahlberg, I. F. J. Vankelecom, P. P. Pescarmona, A. Hubin, *Electrochim. Acta* **2013**, *111*, 405–410.

## Entry for the Table of Contents

# ARTICLE

**The underestimated impact of the composition and preparation of the rotating disk electrode**: The influence of the electrocatalyst loading and of the binder type and content on the ORR performance of doped ordered mesoporous electrocatalysts was investigated and showed to have a relevant impact on product selectivity and kinetic current density (see picture).

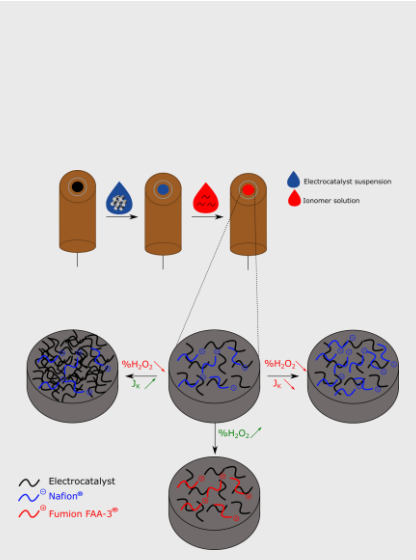


*N. Daems, T. Breugelmans, I.F.J. Vankelecom, P.P. Pescarmona**

***Page No. – Page No.***

***Influence of the composition and preparation of the rotating disk electrode on the performance of mesoporous electrocatalysts in the alkaline oxygen reduction reaction***